CISTER
Research Centre in
Real-Time & Embedded
Computing Systems

Conference Paper

Two-Ray Model Analysis for Overwater Communication at 28 GHz with Different Heights

Miguel Gutiérrez Gaitán
Miguel Gutiérrez Gaitán
Luís Almeida
Luís Almeida

CISTER-TR-231203

2023/12/06

Two-Ray Model Analysis for Overwater Communication at 28 GHz with Different Heights

Miguel Gutiérrez Gaitán, Miguel Gutiérrez Gaitán, Luís Almeida, Luís Almeida

CISTER Research Centre

Rua Dr. António Bernardino de Almeida, 431

4200-072 Porto

Portugal

Tel.: +351.22.8340509, Fax: +351.22.8321159

E-mail: mjggt@isep.ipp.pt, mjggt@isep.ipp.pt, lda@fe.up.pt, lda@fe.up.pt

https://www.cister-labs.pt

Abstract

This research aims to assess the signal propagation behavior of millimeter waves (mmWaves) over maritime environments. It focuses on the path loss performance of shore-to-vessel and vessel-to-vessel overwater communication at 28 GHz when considering line-of-sight conditions. The study is conducted by means of synthetic simulations at four different receiver antenna heights with respect to the water surface, representing emerging maritime Internet-of-Things application scenarios. Simulation results are shown concerning the path loss and the excess path loss 13 additional path loss relative to that in free-space 13 for each particular antenna height, over different TX-RX separations. We also show the cumulative distribution function of the excess path loss. The outcomes reveal variations of up to 10 dB in path loss performance depending on the height-distance setup. The results also reveal an initial distance range for all antenna heights in which the excess path loss is below 3 dB with 90% probability.

© 2023 CISTER Research Center
www.cister-labs.pt

Two-Ray Model Analysis for Overwater Communication at 28 GHz with Different Heights

Jorge Celades-Martínez*, Mauricio Rodríguez*, Miguel Gutiérrez Gaitán†‡ and Luís Almeida‡§

*Pontificia Universidad Católica de Valparaíso, Chile
jorge.celades.m@mail.pucv.cl, mauricio.rodriguez.g@pucv.cl
†Universidad Andres Bello, Chile, miguel.gutierrez@unab.cl
‡CISTER Research Centre, Portugal
mjggt@isep.ipp.pt
§University of Porto, Portugal
lda@fe.up.pt

2023 IEEE MTT-S Latin America Microwave Conference (LAMC) | 979-8-3503-1640-7/23/$31.00 ©2023 IEEE | DOI: 10.1109/LAMC59011.2023.10375603

***Abstract*—This research aims to assess the signal propagation behavior of millimeter waves (mmWaves) over maritime environments. It focuses on the path loss performance of shore-to-vessel and vessel-to-vessel overwater communication at 28 GHz when considering line-of-sight conditions. The study is conducted by means of synthetic simulations at four different receiver antenna heights with respect to the water surface, representing emerging maritime Internet-of-Things application scenarios. Simulation results are shown concerning the path loss and the excess path loss – additional path loss relative to that in free-space – for each particular antenna height, over different TX-RX separations. We also show the cumulative distribution function of the excess path loss. The outcomes reveal variations of up to 10 dB in path loss performance depending on the height-distance setup. The results also reveal an initial distance range for all antenna heights in which the excess path loss is below 3 dB with 90% probability.**

***Index Terms*—Two-Ray, mmWaves, Over Water, Large Scale.**

I. Introduction

The Internet of Things (IoT) paradigm and the fifth-generation (5G) wireless communication systems are revolutionizing network connectivity everywhere. Maritime environments such as coastal zones, harbors, marinas, etc., are rapidly becoming smart and connected, leading to new technological concepts such as The Maritime IoT [1]. Wireless networked systems leveraging 5G and IoT are nowadays more common in water environments [2], supporting both traditional (e.g., aquaculture [3]) and emerging (e.g., smart marinas [4]) applications for the benefit of the blue economy.

Millimeter wave (a.k.a., mmWave) frequency bands have recently been considered as one the candidates for future maritime communications [5]. While its potential benefits for emerging and upcoming high-bandwidth IoT/5G-based applications are promising (e.g., for real-time vessel-to-shore video transmission [6]), the study of the mmWave signal propagation behavior over water areas still remains little explored.

In general, signal reflections on the water surface are stronger than in terrestrial settings, which can lead to severe constructive/destructive interference on the receiver side. This situation can generally be well explained by the two-ray model [7], which can also be used to explain other phenomena that can affect mmWave signal propagation over water. For example, the impact of tides (a.k.a. tidal fading [8]) and occlusion (or shadowing [9]) due to sea waves are also a matter of concern in aquatic areas, especially in IoT-driven scenarios where the typical short to medium range distances and reduced height settings can intensify attenuation effects.

In this work, we investigate the path loss (PL) performance of mmWave signals at 28 GHz targeting IoT-driven overwater communication scenarios in Line-of-Sight (LOS) conditions. To this purpose, we consider both shore-to-vessel (S2V) and vessel-to-vessel (V2V) communication when considering varying TX-RX separations, and different antenna heights. The objective of this study is to obtain large-scale fading statistics for the design of mmWave overwater links that are well described by the two-ray propagation model.

Related Work. Propagation over water is a subject of study that generates interest in the field of telecommunications. Existing literature includes studies evaluating conditions for connecting unmanned surface vehicles (USVs) [10] or autonomous underwater vehicles (AUV) [11] operating at the surface, typically based on transmission links using IEEE 802.11 (WiFi) technologies. In [11], measurements considered two onshore antenna heights to communicate with an AUV equipped with an external antenna at 17 cm height operating within 100 m from the shore. In [10], the operation with the USV considered distances between 50-450 m, and antenna heights of ∼5-6 m for the onshore node, and between ∼0.4-0.5 m on the USV. Both studies agree on the suitability of the two-ray model to predict path loss within the 200 m range. In an urban setting, the work in [12] analyzed the path loss performance of mmWave at 28 GHz while also considering diffraction.

Contributions. This research provides a theoretical study to better understand the large-fading behavior of LoS overwater mmWave communication at 28 GHz. It reveals results for

Authorized licensed use limited to: b-on: UNIVERSIDADE DO PORTO. Downloaded on May 08,2024 at 02:36:38 UTC from IEEE Xplore. Restrictions apply.

different heights to address potential constraints in TX/RX antenna installation and/or due to tidal level shifts. These results shed light on the potential service coverage for IoT-driven scenarios with USVs/AUVs in a myriad of application settings.

II. Channel Model

We consider the two-ray model [13] to perform our theoretical study. This propagation model is particularly suitable to represent scenarios in which a single surface reflection has a dominant effect on multi-path propagation. This aligns well with our LOS S2V and V2V scenarios, in which we consider the effect of two distinct components: a LOS direct ray between the transmitter and the receiver, and an indirect (reflected) ray from the surface (see Fig. 1 for the S2V case). Note that the output of the model is the power received (P_r) resulting from the vectorial summation of the two components, which can be expressed mathematically as follows:

$$P_r = P_t \left[\frac{\lambda}{4\pi}\right]^2 \left|\frac{\sqrt{G_l}}{l} + \frac{R\sqrt{G_r}e^{j\Delta\phi}}{x+x'}\right|^2, \quad (1)$$

where P_t is the transmission power, G_l the product of the TX and RX antenna gains in the LOS direction, G_r the product of the TX and RX antenna gains in the directions of the reflected ray, l the length of the direct ray, $x + x'$ the length of the reflected ray, $\Delta\phi$ the phase difference between the LOS and reflected signals at the receiver, and R the reflection coefficient as:

$$R = \frac{\sin\theta - Z}{\sin\theta + Z} \quad \text{where} \quad Z = \frac{\sqrt{\varepsilon_0 - cos^2\theta}}{\varepsilon_0}.$$

Note we use Z as defined in [14] for vertical polarization, where θ is the angle of incidence of the reflected ray, and $\epsilon_0 = \epsilon - j60\sigma\lambda$ where ϵ is the dielectric constant (relative permittivity) of the reflective medium relative to unity in free space and σ is the conductivity of the reflective medium.

III. Simulation Setup

The simulation setup is summarized in Table I, describing realistic operation conditions for both LOS S2V and V2V overwater communication at 28 GHz. In all cases, both RX and TX are considered to use omnidirectional antennas vertically polarized, separated by a TX-RX (horizontal) distance within the interval $[1, 3000]$ m. In addition, we assume unitary antenna gains.

Concerning the physical properties of the water medium, we assume the dielectric constant and conductivity of typical seawater [14], i.e., $\epsilon = 81$ and $\sigma = 5$ [S/m].

a) Transmitter: The TX is assumed to be mounted on a vehicle (floating) on the water surface. In terms of antenna heights, we consider 0.17 m for all cases, assuming a real-world AUV operating at the surface, as the one described in [15].

b) Receiver: As for the RX antenna height, we considered four different values, namely $\{0.17, 0.5, 1.5, 5.0\}$ m, representing four typical IoT-driven S2V communication scenarios. Among these heights, the first one (0.17 m) also applies for V2V

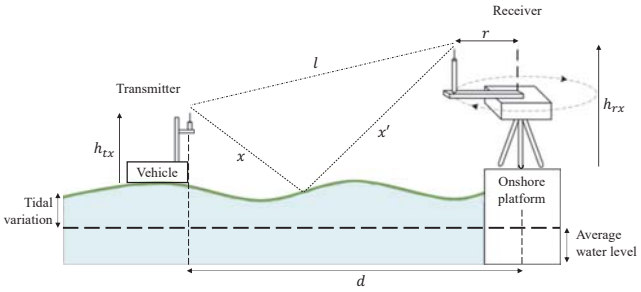

Fig. 1. The two-ray model showing the length l of the direct LOS ray, the length $x + x'$ of the reflected ray that depends on the water level, the horizontal distance d between TX and the center of the rotating arm, and the radius r of the rotating arm that rotates 360 degrees in the horizontal plane with the RX in its tip.

TABLE I. Simulation Specifications

Parameter	Symbol	Value
Frequency	*f*	*28 GHz*
Transmitter height	*htx*	*0.17 m*
Receiver heights	*hrx*	*[0.17, 0.5, 1.5, 5] m*
Transmission Power	*Pt*	*0 dBm*
Transmitter Gain	*Gt*	*0 dBi*
Receiver Gain	*Gr*	*0 dBi*
Permittivity	ϵ	*81*
Conductivity	σ	*5 S/m*
Rotatory Arm	*r*	*0.4 m*
Operational distances	*d*	*[1, 3000] m*

overwater communication, assuming communication among two vessels under calm water conditions (i.e. a flat surface).

c) Rotating arm: The receiver side (onshore) also considers the RX to be installed on an arm that rotates 360 degrees in the horizontal plane (Fig. 1). This setting mimics the behavior of real-world specialized equipment capabilities (as in [16]) whose end goal is to eliminate small-scale fading effects in experimental measurements.

Note that the rotating arm modifies the computation of the effective link distance as follows:

$$d_r = \sqrt{r^2 + d^2 - (2\ r\ d\ \cos\alpha)}, \quad (2)$$

where d_r is the effective TX-RX horizontal distance, r is the arm length, d the horizontal distance between TX and the center of the rotating arm, and α the horizontal angle of the rotating arm with the TX-RX direction.

IV. Simulation Results

This section presents the results achieved with the referred simulation setup. We performed a comprehensive large-scale analysis for the two-ray model at different heights and varying d in the referred range with increments of 0.1 m. For each value of d we computed d_r for a full 360 degrees rotation of the arm holding the RX and averaged the performance metrics, namely: i) path loss (PL), ii) excess path loss (EPL). Then, for clarity, we also present: iii) the CDF of random EPL observations and iv) the percentile 90 of EPL for the considered distance range.

Authorized licensed use limited to: b-on: UNIVERSIDADE DO PORTO. Downloaded on May 08,2024 at 02:36:38 UTC from IEEE Xplore. Restrictions apply.

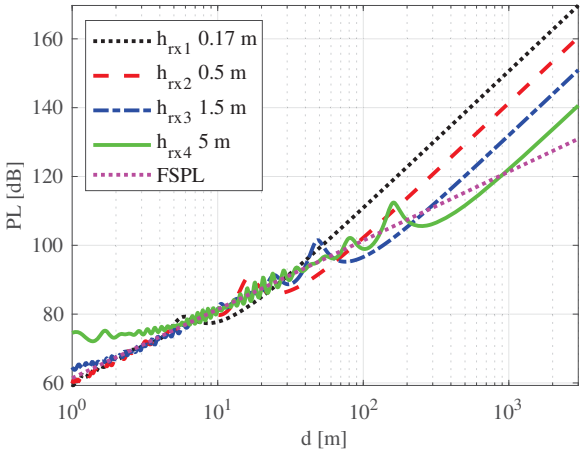

Fig. 2. Path Loss for different h_{rx} and $d \in [1, 3000]$ m

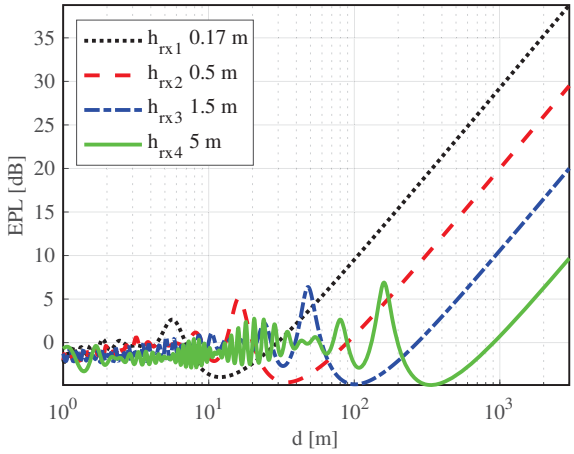

Fig. 3. Excess Path Loss for different h_{rx} and $d \in [1, 3000]$ m

(i) Path Loss. Fig. 2 presents the average PL using the two-ray model at four different antenna heights when varying distances between 1 and 3000 m. The figure also includes the free-space path loss (FSPL) as a reference. By graphical inspection, these results allow us to see a clear difference in the breakpoint (BP) distances (the point at which the loss starts to increase steadily) for each of the four height configurations. Specifically, the BP is about 10 m for a receiver height of 0.17 m, near 30 m for the 0.5 m height, about 100 m for the 1.5 m height, and approximately 300 m for the receiver height at 5 m. After the last BP, we can observe that the difference between each receiver height is about 10 dB.

(ii) Excess Path Loss. With the aim of providing a better understanding of the power loss versus distance, we also considered the difference between the (two-ray) PL and the classical FSPL, and described as follows: $\text{EPL}(d) = \text{PL}(d) - \text{FSPL}(d)$.

Fig. 3 shows EPL vs. distance for the four values of h_{r_x}. As expected, we can see there is a clear non-linear behavior due

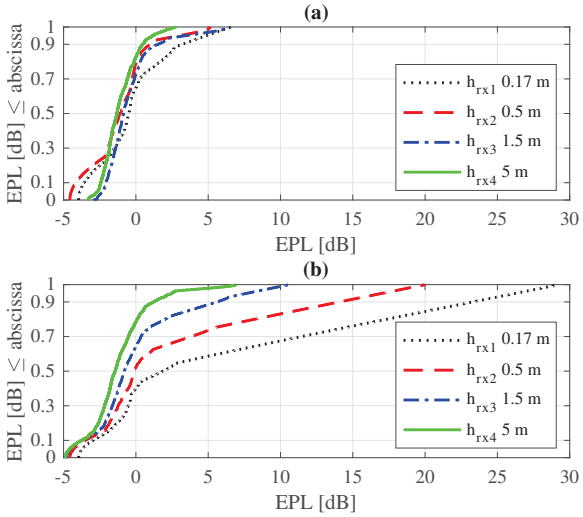

Fig. 4. CDF of EPL at different heights for two coverage distances d. (a): 70 m, (b): 1000 m

to constructive and destructive interference between the direct and reflected rays (variations of l and $x + x'$, as explained by the two-ray model). This situation shows that the interference can change in opposite directions at different heights for each distance. For example, at approximately 170 m of coverage distance, a receiver height of 1.5 m exhibits an EPL of around -4 dB, while a receiver height of 5 m shows an EPL of around 6 dB. This highlights a disparity of near 10 dB between two consecutive receiver heights. Similar observations can be made for receiver heights of 0.17 m and 0.5 m. This is interesting as it shows that higher heights do not always result in lower EPL. In fact, EPL tends to be lower for lower heights within the mentioned short distances.

(iii) CDF of the EPL. To view the probability of a random observation of EPL, we analyzed the cumulative distribution function (CDF) at two distances, namely $d = 70$ m and $d = 1000$ m (Fig. 4). In the first case (on top) we observe that EPL median remains negative (i.e., PL below FSPL) for all receiver heights. However, the percentile 90 reveals an EPL difference between a receiver height of 0.17 m and 5 m of around 3 dB. As the coverage distance increases, receiver heights show higher EPL swings. This can be observed in Fig. 4 bottom, showing a coverage distance of 1000 m. Any percentile above the median shows clear EPL differences between the different heights. Between the receiver heights of 0.17 m and 5 m the EPL varies about 21 dB.

(iv) Percentile 90 of EPL. Finally, we show the variation of the percentile 90 of EPL in the considered distance range (Fig. 5). This shows the expected maximum EPL at each given distance, with 90% probability. The observed behavior is similar for all receiver antenna heights. There is an initial distance range in which the EPL values are below 3 dB with at least 90% probability, followed by a linear increase with the log of the distance. The initial distance range with low EPL increases

Authorized licensed use limited to: b-on: UNIVERSIDADE DO PORTO. Downloaded on May 08,2024 at 02:36:38 UTC from IEEE Xplore. Restrictions apply.

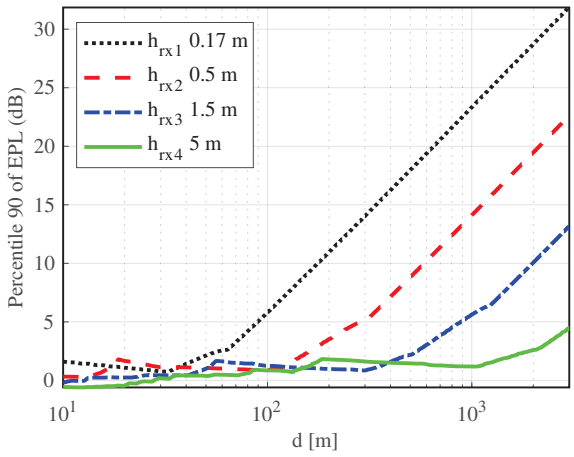

Fig. 5. Percentile 90 of EPL with $d \in [10, 3000]$ m

with the receiver antenna height, from about 70 m for a height of 0.17 m, which represents a V2V scenario with antennas near the reflection surface, to around 150 m for a height of 0.5 m, 400 m at a height of 1.5 m and 1000 m at a height of 5 m, these last cases representing typical S2V scenarios.

V. Conclusion

This research presents a comprehensive analysis of millimeter wave propagation in aquatic environments, focusing on the evaluation of PL and EPL at different receiver heights. Through extensive simulations, we obtained valuable insights into the performance of wireless mmWave communication in distinctive maritime settings. Our findings reveal distinct trends in signal behavior at varying receiver heights and distances. The study highlights the significance of the antenna height at each distance to determine the path loss in the wireless link. This observation shows an opportunity to compensate the impact of variations in antenna height, whether due to installation constraints or tide changes. Furthermore, it is worth noting that the EPL values remain relatively small for an initial range of the coverage distance, meaning the link loss in this range is similar to that observed in free space. This range is relatively short for V2V scenarios (we observed about 70 m), but it can grow to near 1000 m for S2V scenarios. After this initial range, the EPL grows steadily at a similar rate for all antenna heights. In future work, we will carry out an empirical validation of these findings, using practical implementations of mmWave wireless communication systems in maritime environments, and extend the analysis to incorporate the influence of sea waves and tidal dynamics. Overall, we aim at contributing to the design of robust, efficient, and smarter maritime communication solutions.

References

[1] T. Xia, M. M. Wang, J. Zhang, and L. Wang, "Maritime Internet of Things: Challenges and solutions," *IEEE Wireless Communications*, vol. 27, no. 2, pp. 188–196, 2020.

[2] A. Zolich, D. Palma, K. Kansanen, K. Fjørtoft, J. Sousa, K. H. Johansson, Y. Jiang, H. Dong, and T. A. Johansen, "Survey on communication and networks for autonomous marine systems," *Journal of Intelligent & Robotic Systems*, vol. 95, pp. 789–813, 2019.

[3] R. W. Coutinho and A. Boukerche, "Towards a novel architectural design for IoT-based smart marine aquaculture," *IEEE Internet of Things Magazine*, vol. 5, no. 3, pp. 174–179, 2022.

[4] T. Savić, K. Brun-Laguna, and T. Watteyne, "Blip: Identifying boats in a smart marina environment," in *DCOSS 2023-19th International Conference on Distributed Computing in Sensor Systems*, 2023.

[5] F. S. Alqurashi, A. Trichili, N. Saeed, B. S. Ooi, and M.-S. Alouini, "Maritime communications: A survey on enabling technologies, opportunities, and challenges," *IEEE Internet of Things Journal*, 2022.

[6] T. Zugno, F. Campagnaro, and M. Zorzi, "Controlling in real-time an ASV-carried ROV for quay wall and ship hull inspection through wireless links in harbor environments," in *Global Oceans 2020: Singapore–US Gulf Coast*. IEEE, 2020, pp. 1–9.

[7] M. G. Gaitán, P. M. Santos, L. R. Pinto, and L. Almeida, "Experimental evaluation of the two-ray model for near-shore WiFi-based network systems design," in *2020 IEEE 91st Vehicular Technology Conference (VTC2020-Spring)*. IEEE, 2020, pp. 1–3.

[8] A. Macmillan, M. K. Marina, and J. T. Triana, "Slow frequency hopping for mitigating tidal fading on rural long distance over-water wireless links," in *2010 INFOCOM IEEE Conference on Computer Communications Workshops*. IEEE, 2010, pp. 1–5.

[9] Y. Huo, X. Dong, and S. Beatty, "Cellular communications in ocean waves for maritime Internet of Things," *IEEE Internet of Things Journal*, vol. 7, no. 10, pp. 9965–9979, 2020.

[10] A. Coelho, M. Lopes, B. Ferreira, R. Campos, and M. Ricardo, "Experimental evaluation of shore to unmanned surface vehicle wi-fi communications," in *2018 Wireless Days (WD)*. IEEE, 2018, pp. 86–91.

[11] M. G. Gaitán, P. M. d'Orey, P. M. Santos, M. Ribeiro, L. Pinto, L. Almeida, and J. B. De Sousa, "Wireless radio link design to improve near-shore communication with surface nodes on tidal waters," in *OCEANS 2021: San Diego–Porto*. IEEE, 2021, pp. 1–8.

[12] X. Liao, X. Li, Y. Wang, J. Zhou, T. Zhao, and J. Zhang, "Path loss modeling in urban water–land environments at 28 GHz: Considering water surface reflection and building diffraction," *IEEE Antennas and Wireless Propagation Letters*, vol. 22, no. 4, pp. 744–748, 2022.

[13] A. Goldsmith, *Wireless communications*. Cambridge university press, 2005.

[14] W. C. Jakes and D. C. Cox, *Microwave mobile communications*. Wiley-IEEE press, 1994.

[15] P. M. d'Orey, M. G. Gaitán, P. M. Santos, M. Ribeiro, J. B. Sousa, and L. Almeida, "Empirical evaluation of short-range WiFi vessel-to-shore overwater communications," in *Proceedings of the 16th ACM Workshop on Wireless Network Testbeds, Experimental evaluation & CHaracterization*, 2022, pp. 77–84.

[16] M. Rodriguez, R. Feick, H. Carrasco, R. Valenzuela, M. Derpich, and L. Ahumada, "Wireless access channels with near-ground level antennas," *IEEE Transactions on Wireless Communications*, vol. 11, no. 6, pp. 2204–2211, 2012.

Authorized licensed use limited to: b-on: UNIVERSIDADE DO PORTO. Downloaded on May 08,2024 at 02:36:38 UTC from IEEE Xplore. Restrictions apply.